Isomer Identification for Fullerene C_{84} by ^{13}C NMR Spectrum: A Density-Functional Theory Study

Guangyu Sun and Miklos Kertesz*

Department of Chemistry, Georgetown University, 37th and O Streets, NW, Washington, D.C. 20057-1227

Received: March 5, 2001

Optimized geometries of all 24 isolated pentagon rule (IPR) abiding isomers of fullerene C_{84} have been calculated using density-functional theory (DFT) at the B3LYP/6-31G* level. ^{13}C NMR chemical shieldings are obtained employing the gauge-independent atomic orbital method. The calculated chemical shifts are in good agreement with experimental values for isomers **4**, **22**, and **23**, all of which have been experimentally assigned without ambiguity. The calculated NMR spectra allow us to confirm earlier assignment and validate the DFT approach. The previously temporarily assigned isomers D_2(II), C_2, C_s(a), and C_s(b) are isomers **5**, **11**, **16**, and **14**, respectively. Discrepancies exist between the experimental and theoretical NMR spectra for isomers **19** and **24**. The predicted NMR spectra for other isomers are also presented. The local geometry is determined largely by connectivity. The relationship between the chemical shift and the π-orbital axis vector (POAV) angle is far from linear, although the chemical shift generally increases when the POAV angle increases. The pyrene-type carbons form five distinct groups in the chemical shift vs POAV angle graph according to the local connectivity, providing a usable tool for their identification. Similarly, two and three groups can be identified for corannulene and pyracylene types of carbons, but these are not sufficiently distinct to be useful.

I. Introduction

Research on fullerene C_{84} has been active since the starting days of fullerene chemistry, because it is one of the main components[1] of fullerene soot beyond C_{60} and C_{70}. Studies that have been performed on either isomer-pure or mixture samples include potassium intercalation,[2] vapor pressure,[3] vibrational spectroscopy,[4] and chemical reactivity,[5] which add to our knowledge on physical properties of fullerene C_{84}. On the other hand, the exploration of isomers of C_{84} is still an intriguing problem, because, although a number of C_{84} isomers have been identified, more isomers remain to be discovered and identified.

Under the isolated pentagon rule (IPR),[6] fullerene C_{84} has 24 possible isomers.[7] Two major isomers out of the 24 possible IPR isomers have been observed by ^{13}C NMR spectroscopy in mixture.[8−10] Formed in the ratio of 2:1, these isomers have D_2 and D_{2d} point-group symmetry. On the basis of the NMR pattern, the D_{2d} isomer was determined[8−10] as isomer **23**, after the nomenclature of Manolopoulos and Fowler.[7] Figure 1 shows the observed C_{84} isomers. The D_2 isomer proved to be isomer **22** by 2D NMR measurement on the ^{13}C-enriched sample.[11] By means of recycling HPLC, these two isomers have been separated and each characterized by ^{13}C NMR measurement.[12] An early attempt to characterize minor C_{84} isomers presented in the main and tail HPLC fractions yielded about 150 NMR lines,[4a] which posed great difficulties for identification of the minor isomers. Two minor isomers possessing high symmetry were separated from other isomers and characterized to be **24** and **19**.[13] Most recently, Dennis et al.[14] achieved the separation of five minor isomers that have C_2, C_s, C_s, D_{2d}, and D_2 symmetry in a multistage recycling HPLC study. Of the five newly isolated isomers, the D_{2d} isomer can be unambiguously identified as isomer **4**, whereas the others can only be assigned temporarily using point-group symmetries. The separation of C_{84} isomers via chemical reaction has also been reported.[5,15]

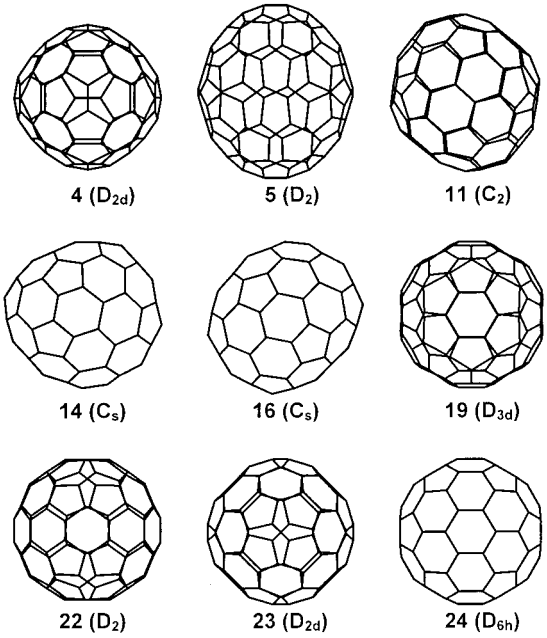

Figure 1. Nine observed IPR isomers of fullerene C_{84}. The group symmetries are given in parentheses. Isomer numbering follows ref 7.

On the theoretical side, much effort has been devoted to the relative stability of C_{84} isomers after the 24 IPR isomers of C_{84} were enumerated[7] in 1992. Using a tight-binding molecular-dynamics (TBMD) scheme, the first complete survey of C_{84} isomers suggested that isomers **22** and **23** have similar energy values and are the most stable ones.[16] Shortly thereafter,

* To whom correspondence should be addressed. Phone: (202)-687-5761. Fax: (202)-687-6209. E-mail: kertesz@georgetown.edu.

10.1021/jp0108418 CCC: $20.00
Published on Web 04/28/2001

semiempirical calculations using various parametrizations including MNDO, AM1, and PM3 showed similar results.[17] SCF calculation employing a split-valence basis set confirmed that isomers **22** and **23** are essentially iso-energetic.[18] The isomer stability yielded by quantum consistent force field for π electrons (QCFF/PI)[19] is in overall agreement with earlier results. Subsequent calculations using various methods including SCF/DZ//MNDO,[20] BP86/3-21G,[20] HF/3-21G,[21] and the density-functional-based tight-binding (DFTB) method[22] all show that isomers **22** and **23** are essentially iso-energetic and more stable than others by at least 6 kcal/mol. A recent study utilizing the density-functional theory (DFT) at the B3LYP/6-31G* level confirmed earlier theoretical findings.[23]

The numbers and intensities of NMR peaks for the C_{84} isomers based on topological symmetry were listed in ref 7. Because more than one isomer may have the same symmetry and similar NMR patterns would be expected, accurate chemical shifts are needed for identifying isomers possessing the same symmetry. An early attempt to predict ^{13}C NMR shifts for C_{84} by Hartree−Fock (HF) approximation was made by Schneider et al.[18] On the basis of calculations on isomers **5**, **22**, and **23** and estimation on isomer **1**, isomers **1** and **5** were eliminated as candidates for the observed D_2 isomer by comparing the range of calculated chemical shifts with the experimentally observed range. Heine et al calculated the chemical shifts of isomers **1**, **5**, **21**, **22**, and **23** using the DFTB method.[24] Their results supported the experimental assignment of the major isomers on the basis of total energy and spectral span. Latter on, the NMR spectra of all of the 24 IPR isomers of C_{84} were calculated using the DFTB method.[22] We have recently employed DFT at the B3LYP/6-31G* level to calculate chemical shifts for three isomers: **21**−**23**, which allowed us to confirm isomers **22** and **23** are the experimentally observed ones.[25] The B3LYP/6-31G* approach also proved to give sufficiently accurate chemical shifts for fullerenes C_{60}, C_{70}, C_{76}, C_{78},[26] C_{80},[27] and C_{82}.[28]

In this work, we have calculated ^{13}C NMR chemical shifts for all of the 24 IPR isomers of fullerene C_{84} by DFT. For isomers already unambiguously assigned, **4**, **22**, and **23**, our calculations show good agreement with the experimental NMR spectra. On the basis of the good agreement between our prediction and the experimental spectra, the molecular structures of the other four experimentally observed isomers, C_2, C_s(a), C_s(b), and D_2, are assigned. For isomers not yet observed, theoretical NMR chemical shifts are given and could be useful in their identification once the isomers become available. The effect of connectivity on local geometry and chemical shift is also studied for the observed isomers.

II. Computational Methods

Full geometry optimizations and NMR chemical shielding calculations are performed on the 24 IPR isomers of C_{84}. Becke's three-parameter (B3)[29] hybrid functional incorporating exact exchange in combination with Lee, Yang, and Parr's (LYP)[30] correlation functional is used throughout this study. Three basis sets STO-3G, 3-21G, and 6-31G* are used in this sequence for geometry optimizations in order to minimize computation time as well as to get energy values at different theory levels. To ensure the calculated structures are indeed minima, geometry optimizations and vibrational analyses are performed using the PM3 semiempirical method. The optimized structure of isomer **10** shows one imaginary frequency, which is confirmed by a B3LYP/STO-3G calculation. The displacement vector of the imaginary frequency indicates that the structure distorts to C_1 symmetry. Therefore, isomer **10** is not included in subsequent calculations.

The 6-31G* basis set is used in chemical shielding calculations upon the recommendation by Cheeseman et al.[31] and our own experience.[25−27] The isotropic NMR chemical shielding constants are evaluated at the B3LYP/6-31G* optimized geometry employing the gauge-independent atomic orbital (GIAO) method.[32] The calculated chemical shielding constants are then referenced to that of C_{60}, using an experimental chemical shift[4a] of 143.15 ppm, to get the chemical shifts. Reference 26 gives a detailed discussion. Geometry optimizations are carried out using Gaussian 98,[33] and NMR calculations are performed using the PQS[34] suite of ab initio programs.

III. Results and Discussion

Geometry and Energy. The minimum, maximum, and average bond lengths of every isomer optimized at the B3LYP/6-31G* level as well as the relative energies obtained by different basis sets are summarized in Table 1 for all C_{84} isomers. The calculated molecular total energy was used without zero-point energy correction. Also listed are energy values obtained by earlier theoretical studies.

Isomers having higher energy values show slightly shorter minimum bond lengths or slightly longer maximum bond lengths. The average bond lengths are all within the narrow 1.4323∼1.4330 Å range. Our predicted energies are in agreement with the earlier results. Isomers **22** and **23** have almost the same energy. Isomers **4**−**6**, **11**, **12**, **14**−**16**, **18**, **19**, **21**, and **24** have energy values that are less than 20 kcal/mol above isomer **23** at the B3LYP/6-31G* level of theory, indicating that these isomers could be the first to be observed. On the contrary, isomers **1**−**3** and **20** have energy values higher than 30 kcal/mol, showing them very unstable.

Because kinetic stability plays an important role in the process of fullerene formation, we try to address it using the calculated HOMO−LUMO gap. It has been shown that Kohn−Sham orbitals and eigenvalues[35] are useful similarly to traditional HF molecular orbitals and energies.[36,37] Weighted HOMO−LUMO gaps calculated by the Hückel method have been used to address the kinetic stability of fullerenes.[38] Here we use the HOMO−LUMO gap as a zero-order approximation to the kinetic stability of C_{84} isomers. The HOMO−LUMO gaps calculated at the B3LYP/6-31G* level of theory are listed in Table 1. The calculated HOMO−LUMO gaps spread over a wide range, varying from 2.65 eV for isomer **20** to 0.79 eV for isomer **3**. The stability of the isomers can be well explained by the combination of relative energy and HOMO−LUMO gap.

NMR Chemical Shifts. The predicted ^{13}C NMR chemical shifts for the C_{84} isomers are listed in Table 2 in numerically increasing order. The predicted NMR spectra are also shown in Figures 2−8 and compared to the experimental spectra when available. Both theoretical and experimental spectra are presented as sticks. We note that the chemical shifts may have very close values in the calculations and/or in the experiments, which makes the spectra appear to have fewer peaks than they should have. In those cases, the values in Table 2 should be consulted. In the following section, we will group the isomers according to their symmetry and discuss the predicted and the experimental NMR spectra in detail.

A. D_{2d} Isomers. One of the D_{2d} isomers, isomer **23**, is one of the two most abundant isomers of C_{84}, and its identification has been long established.[8−10,12] The other D_{2d} isomer, **4**, has also been observed in the experiment.[14] Because their NMR patterns differ in the numbers of full-intensity peaks and half-intensity peaks, these two isomers can be identified without ambiguity, thus, serving as testing cases to illustrate the accuracy of our theoretical results.

TABLE 1: Bond Length Statistics and Relative Energies of the 24 IPR Isomers of C_{84}[a]

	isomer[b]	shortest R_{cc}	longest R_{cc}	average R_{cc}	B3LYP/ STO-3G	B3LYP/ 3-21G	B3LYP/ 6-31G*[c]	HOMO−LUMO[d]	TB-MD[e]	PM3[f]	HF[g]	QCFF/ PI[h]	SCF/ DZ[i]	BP86/ 3-21G[j]	HF/ 3-21G[k]	DFTB[l]
D_2	1	1.356	1.471	1.4330	55.59	42.92	51.53	2.37	43.2	46.2		60.6			45.8	54.3
C_2	2	1.356	1.472	1.4326	36.55	28.24	32.91	1.95	28.0	32.7		43.9			32.9	34.4
C_s	3	1.367	1.480	1.4327	35.40	30.91	31.97	0.79	20.5	34.5		36.6				24.4
D_{2d}	**4**	1.373	1.476	1.4324	16.76	13.10	14.64	2.13	14.0	18.3		26.1	22.6	11.3	18.1	15.5
D_2	**5**	1.376	1.471	1.4323	19.01	14.50	15.94	1.91	14.9	19.2	23.8	28.0			21.2	15.3
C_{2v}	**6**	1.365	1.473	1.4326	17.78	14.09	17.06	1.37	11.3	13.9		17.3	20.1			15.8
C_{2v}	7	1.361	1.477	1.4327	27.67	23.69	24.50	1.30	14.9	24.3		23.7				20.6
C_2	8	1.364	1.473	1.4325	25.42	21.64	22.03	0.99	12.9	30.7		28.5			38.2	17.4
C_2	9	1.361	1.474	1.4326	29.66	26.14	26.30	0.81	16.4	31.6		28.4			40.1	22.0
C_s	10				35.09[m]		28.7[n]		14.4	37.1		36.2				18.9
C_2	**11**	1.365	1.471	1.4325	8.69	6.95	8.39	1.64	5.5	7.2		7.8	9.7		7.8	7.9
C_1	**12**	1.361	1.475	1.4325	13.88	12.08	12.20	1.46	6.9	13.0		11.9	17.7			9.8
C_2	13	1.360	1.477	1.4327	27.86	24.46	24.84	1.16	15.1	25.6		24.1			33.9	20.3
C_s	**14**	1.363	1.472	1.4326	15.73	12.58	14.98	1.91	11.6	14.0		15.9	17.4			15.3
C_s	**15**	1.362	1.473	1.4325	13.00	11.07	11.21	1.54	7.5	12.8		12.1	17.1			9.3
C_s	**16**	1.363	1.473	1.4326	8.23	6.75	8.04	1.78	5.9	6.9		6.4	7.8			8.6
C_{2v}	17	1.360	1.473	1.4328	23.00	20.15	21.63	1.37	15.1	19.4		18.3				20.6
C_{2v}	**18**	1.359	1.470	1.4327	15.79	13.34	15.69	1.96	13.2	12.9		14.0	15.1			17.4
D_{3d}	**19**	1.365	1.468	1.4326	10.35	8.66	10.10	1.39	6.1	7.3		6.5	9.9	11.5		9.6
T_d	20	1.359	1.468	1.4330	31.04	26.01	30.73	2.65	26.5	25.8		29.0	30.5	25.2		34.2
D_2	**21**	1.366	1.475	1.4325	19.31	17.24	16.12	1.35	9.1	18.9		16.2	26.1		26.6	12.7
D_2	**22**	1.367	1.472	1.4324	0.21	0.33	0.08	1.98	−0.8	0.4	0.4	−0.4	0.3	1.4	0.5	−0.5
D_{2d}	**23**	1.367	1.471	1.4324	0.00	0.00	0.00	2.05	0.0	0.0	0.0	0.0	0.0	0.0	0.0	0.0
D_{6h}	**24**	1.368	1.472	1.4326	7.58	6.29	7.08	2.34	6.3	6.8		5.5	6.3	7.7		8.8

[a] Bond lengths in Å. Energy in kcal/mol relative to that of **23** (D_{2d}). [b] Isomers having relative energy less than an arbitrary value of 20 kcal/mol at the B3LYP/6-31G* level are in bold. [c] Similar values were obtained in ref 23. [d] HOMO−LUMO gap (in eV) calculated by B3LYP/6-31G*. [e] Tight binding molecular dynamics, taken from ref 16. [f] Taken from ref 17. [g] (7s4p)[3s/2p] basis set, taken from ref 18. [h] Quantum consistent force field for π electrons, taken from ref 19. [i] SCF/DZ energy at the MNDO geometry, taken from ref 20. [j] Taken from ref 20. [k] Taken from ref 21. [l] Density-functional-based tight-binding method, taken from ref 22. [m] First-order saddle point at the B3LYP/STO-3G level. [n] Taken from ref 23.

Isomer **23** is predicted as the most stable isomer among the 24 IPR isomers of C_{84}. It also has a large HOMO−LUMO gap (2.05 eV), indicating kinetic stability. The predicted NMR pattern for isomer **23** has been described earlier.[25] When compared with the experiment in Figure 2, the spectral span and the relative position of the half-intensity peak with respect to those of full-intensity peaks are both well reproduced in our calculation. Five sets of peaks, with four sets each containing 1, 2, 6, and 1 full-intensity peaks from downfield to upfield and one set containing the half-intensity peak, are also in agreement with experiment.

Isomer **4** is 14.64 kcal/mol less stable than isomer **23**. Its HOMO−LUMO gap, 2.13 eV, is among the largest. The predicted NMR pattern of isomer **4** agrees with the experimental data very well, as shown in Figure 2. In the upfield region, three distinct full-intensity peaks are predicted at 132.15, 135.21, and 137.35 ppm, whereas experimentally, three peaks occur at 131.36, 133.34, and 135.87 ppm. Although in most cases we could not assign each peak, these two sets probably correspond to each other on a one-to-one basis. In the downfield region, six full-intensity peaks form three groups each containing 1, 4, and 1 peaks from downfield to upfield, matching experimental data very well. All of the three half-intensity peaks are predicted to occur above 140 ppm, which also agrees with the experiment. The chemical shifts of the half-intensity peaks differ from the experimental values by up to 1.56 ppm for the experimental peak at 142.54 ppm. This magnitude of the underestimation is much larger than that of the full-intensity peaks in this region. The reason the half-intensity peaks are not as accurately predicted as the full-intensity peaks is not obvious to us.

Overall, our calculations were able to rather accurately reproduce the NMR patterns of the two D_{2d} isomers. The general trend where the peaks above 140 ppm are better reproduced than the peaks below 140 ppm can be seen in these two isomers and in the following cases. An earlier attempt[22] to predict the NMR chemical shifts for C_{84} isomers using the scaled IGLO-DFTB model failed particularly in the case of isomer **4**, in that, one full-intensity peak instead of three peaks appears in the upfield region.

B. D_2 Isomers. Because one of the two major isomers has D_2 symmetry, the four D_2 isomers of C_{84}, **1**, **5**, **21,** and **22**, have been subjected to several theoretical studies.[18,22,24] Combined with energy arguments, these studies support the experimental assignment of isomer **22** as the observed D_2 isomer. We have recently demonstrated that DFT at the B3LYP/6-31G* level is able to distinguish isomers **21** and **22** solely based on NMR chemical shifts.[25]

The calculated NMR spectra of the four D_2 isomers are compared with the experimental data in Figure 3. Isomer **22** is essentially isoenergetic to isomer **23** and has a 1.98 eV HOMO−LUMO gap. The calculated NMR peaks for isomer **22** form five groups, each containing 5, 2, 12, 1, and 1 peaks from downfield to upfield, which agrees with experiment. When listed in numerical order, the calculated chemical shifts give an rms deviation[25] of 0.441 ppm when compared with the experiment.

Isomer **5** has a relative energy of 15.94 kcal/mol and a HOMO−LUMO gap of 1.91 eV, indicating its relatively high stability. Along with its high stability, our theoretical NMR spectrum supports the tentative assignment[14] of the other observed D_2 isomer as D_2(II), or isomer **5**. The most obvious feature of the experimental NMR spectrum of this isomer is the isolated single peak at 151.48 ppm. Other features include the four peaks in the upfield region and the crowded middle part of the spectrum. Our calculated NMR spectrum of isomer **5** shows all these features, which the calculated spectra of isomers **1** and **21** lack. The general trend where the peaks below 140 ppm are overestimated by up to 2 ppm is also seen here clearly.

Isomer **1** has too high of an energy, whereas isomer **21** has too low of a HOMO−LUMO gap, making them less likely to

TABLE 2: ^{13}C Chemical Shifts of C_{84} Isomers Calculated Using B3LYP/6-31G*[a]

1	2	3	4	5	6	7	8	9	11	12	12 cont.	13	14	15	16	17	18	19	20	21	22	23	24
128.94	128.93	104.73	132.15	129.90	133.54	130.04	129.84	118.70	133.77	131.72	140.29	123.10	132.22[b]	132.72[b]	134.76	130.69	136.37	131.16	136.35	132.33	134.25	135.59	136.03[b]
130.20	131.16	112.83	135.21	132.62	133.93	130.86	130.67	119.52	134.05	132.38	140.46	124.45	133.50	133.16	134.89	131.73	136.61	133.85[b]	140.32[b]	133.63	136.25	138.25	139.34[b]
130.61	131.87	123.03	137.35	133.80	134.04	132.96	130.72	119.75	134.10	132.67	140.60	126.73	133.71	134.88	136.12[b]	133.89	136.65	136.86[b]	142.98	133.46	137.16	138.91	140.10
132.42	132.09	125.04	140.98[b]	136.24	134.08	135.11	133.46	127.73	134.39	134.25	140.78	127.40	135.75	135.34	136.17	135.39	136.78	137.44	145.59	134.29	137.50	139.26[b]	140.98[b]
135.89	132.22	127.10	143.48	139.24	134.92	135.42	134.26	127.96	135.42	134.40	141.02	131.20	136.08	135.65	136.50	136.36	137.40	140.30		134.58	138.60	139.47	146.95
135.96	132.70	127.24	144.80[b]	139.67	135.40[b]	135.43	134.86	128.22	135.42	134.44	141.10	131.59	136.19	135.87	136.87	136.43[b]	137.41	141.12		134.45	138.93	139.79	
136.62	132.93	128.44	145.17	140.45	137.18	137.53	135.22	128.96	135.77	134.66	141.13	131.63	136.99	135.95	137.17	136.61	137.57	145.37		137.50	138.48	140.11	
137.72	134.96	129.85	145.80	140.49	138.45	138.73	136.19	132.39	136.19	134.84	141.27	131.72	137.07	136.10	137.50	136.81	138.90[b]	150.95		137.70	138.98	139.98	
141.01	135.25	130.13	146.32	140.62	139.02	138.86	137.12	132.69	136.40	135.10	141.81	131.87	137.49	136.63	137.58	136.85	139.14			139.50	139.09	140.97	
141.76	135.70	131.11	146.83	141.25	139.10	139.93[b]	138.31	133.12	136.48	135.28	141.95	132.43	138.69	136.78	137.61	137.25	139.16			139.14	139.80	141.40	
145.06	137.31	131.30	148.35	141.54	139.96	140.57	138.33	135.94	136.52	135.45	141.96	132.89	139.47	136.97	137.82	137.34	139.78[b]			141.31	140.73	144.51	
145.65	138.59	131.74	148.70[b]	141.75	140.82	140.87	139.06	136.89	136.67	135.48	142.07	133.43	139.87	138.29	138.00	138.74[b]	139.80			141.71	140.76		
145.79	138.65	132.82		141.95	142.69	141.23	139.50	137.05	137.15	135.49	142.21	133.56	139.94	138.48	138.10	138.96[b]	140.79			141.74	140.91		
147.03	138.83	133.08[b]		142.45	142.73	142.05[b]	140.08	137.62	137.47	135.60	142.28	134.36	140.02	138.79	138.24	140.35[b]	140.84			141.79	140.64		
148.40	139.79	133.50		142.65	143.05	142.81	140.16	138.26	137.79	135.63	142.60	134.79	140.03	138.81	138.58	140.41	141.45			142.22	141.93		
148.88	140.14	134.28		143.58	143.32	143.05	140.53	138.29	139.04	135.80	142.87	135.17	140.06	138.87	138.75	140.51	142.58			142.23	142.15		
149.68	140.86	137.07		143.64	143.37	143.70	140.58	138.94	139.18	136.06	143.02	135.72	140.10	139.40	138.80	141.67	142.87			143.41	143.60		
149.76	141.17	137.21		144.48	144.27[b]	144.29	140.79	139.24	139.28	136.11	143.10	137.31	140.42	139.46	139.01	144.05	143.38			143.88	143.73		
149.86	141.29	137.82		144.69	145.73	145.25	140.85	139.72	139.44	136.15	143.13	137.46	140.45	139.49	139.12	144.67[b]	146.73			145.50	144.14		
152.71	141.70	137.84		145.16	145.95[b]	147.09	141.68	139.86	139.56	136.38	143.19	138.07	140.50	139.65	139.22	144.80	146.73			145.75	144.45		
153.84	141.92	139.08		151.07	145.97	147.52[b]	142.93	140.56	139.72	136.54	143.33	138.51	140.50	139.94[b]	139.43	146.27	147.18			146.32	144.58		
	142.19	140.65			148.92	148.16	143.09	141.48	140.97	137.07	143.63	139.07	140.78	140.18	139.71	148.57	148.64						
	142.29	140.77			157.78[b]	158.14[b]	143.66	141.51	140.97	137.11	143.79	139.13	141.01	140.30	139.72	150.50							
	143.24	141.31					143.71	141.60	141.31	137.30	143.85	139.63	141.30	140.36	140.13	152.24							
	143.44	141.67					143.76	141.92	141.49	137.34	143.85	139.82	142.25	140.95[b]	140.48								
	143.76	141.72					145.09	143.27	141.67	137.54	144.55	139.95	142.45	141.37	140.71								
	143.97	141.73					145.29	143.84	141.82	137.66	145.20	140.55	143.05	141.61	141.01[b]								
	144.32	142.78					146.04	143.94	141.88	137.75	146.09	140.57	143.49	142.05	141.14								
	144.35	142.80					147.83	144.40	142.07	137.76	146.22	141.66	143.82	142.11	141.30								
	144.39	143.15					148.47	144.85	142.84	137.87	146.32	142.01	143.86	142.22	141.44								
	144.45	143.19					148.75	147.38	142.98	137.99	146.38	143.58	143.88	142.80	141.82								
	145.70	145.02					149.76	147.85	143.09	138.37	146.57	144.21	143.92	142.84	142.56								
	147.10	145.03					150.50	147.88	144.61	138.56	146.60	144.22	144.71	143.40	143.40								
	147.96	146.58					150.71	149.30	144.84	138.83	146.92	144.27	144.99	143.55	143.70								
	148.35	148.58					150.82	149.42	144.87	138.92	147.10	145.00	145.21	143.89	145.34								
	148.46	148.93					150.90	149.79	144.89	139.04	147.19	146.13	145.53	144.46	145.51								
	150.21	151.48					151.35	149.88	145.41	139.12	147.34	146.98	145.68	144.72	146.20								
	150.34	151.73[b]					153.23	150.17	147.49	139.13	148.04	148.01	145.98	144.83	146.38								
	151.24	153.00					153.88	152.06	147.54	139.60	148.65	148.74	145.99	144.94	147.58								
	151.84	155.02					154.12	153.04	147.69	140.08	149.61	148.83	146.02	145.52	148.53								
	152.27	156.09					155.49	154.14	147.84	140.09		149.81	147.74	147.36	148.57								
	152.64	158.47[b]					158.47	154.98	148.92	140.11		151.53	147.88	149.74	149.02								
		160.74[b]								140.28			148.49[b]	150.76[b]	149.14								
		160.85								140.29				151.58									

[a] Chemical shifts, in ppm, are referenced to that of C_{60} at 143.15 ppm. [b] Peaks with half-intensity.

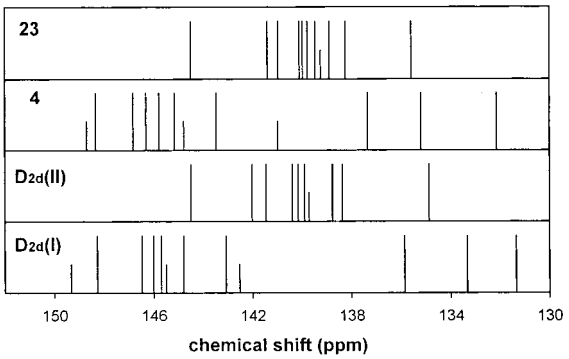

Figure 2. Experimental[12,14] and theoretical ^{13}C NMR spectra of D_{2d} isomers of fullerene C_{84}. Theoretical spectra are labeled by isomer number[7] and experimental spectra labeled by symmetry.

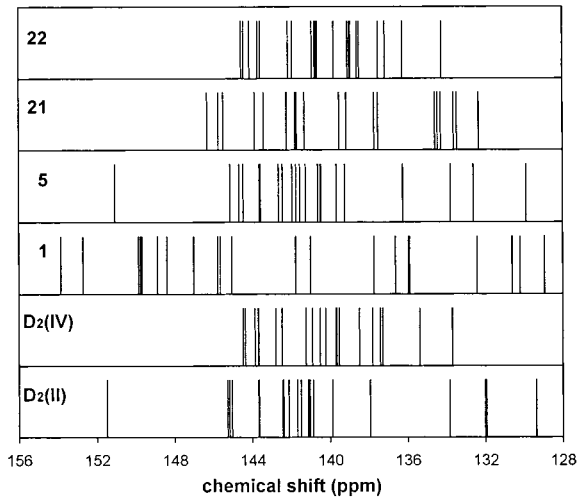

Figure 3. Experimental[12,14] and theoretical ^{13}C NMR spectra of D_2 isomers of fullerene C_{84}. Theoretical spectra are labeled by isomer number[7] and experimental spectra labeled by symmetry.

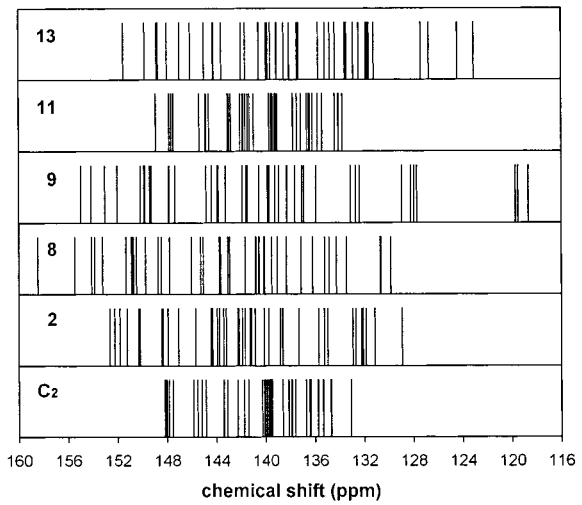

Figure 4. Experimental[14] and theoretical ^{13}C NMR spectra of C_2 isomers of fullerene C_{84}. Theoretical spectra are labeled by isomer number[7] and experimental spectra labeled by symmetry.

be observed. The predicted NMR spectrum of isomer **1** shows the largest spectral span among the four D_2 isomers, whereas isomer **21** has a spectral span only slightly larger than that of isomer **22**. Overall, the NMR peaks of isomers **1** and **21** spread along the entire spectral range. An earlier theoretical study predicted isomer **5** to be less stable by 2.63 kcal/mol[22] than

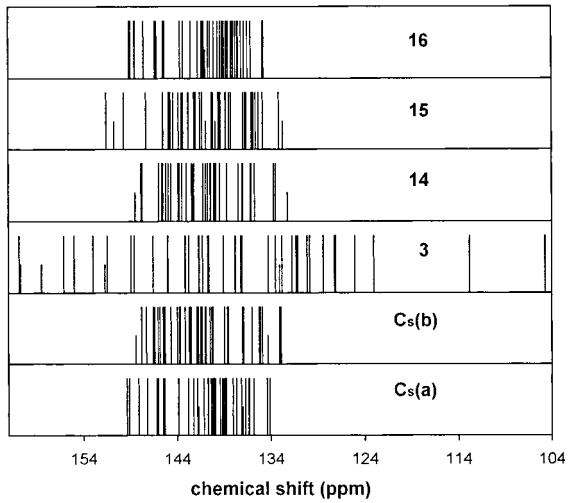

Figure 5. Experimental[14] and theoretical ^{13}C NMR spectra of C_s isomers of fullerene C_{84}. Theoretical spectra are labeled by isomer number[7] and experimental spectra labeled by symmetry.

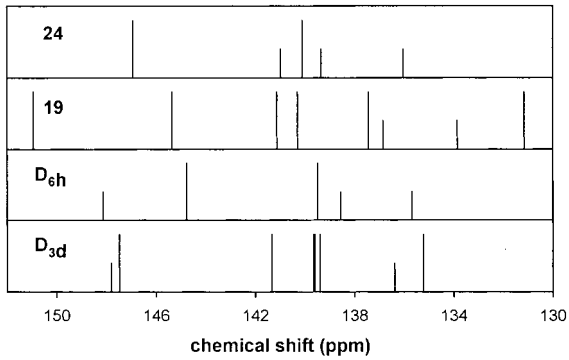

Figure 6. Experimental[13] and theoretical ^{13}C NMR spectra of D_{3d} and D_{6h} isomers of fullerene C_{84}. Theoretical spectra are labeled by isomer number[7] and experimental spectra labeled by symmetry. Spectra adjusted so that the full-intensity peaks show same height in different spectra.

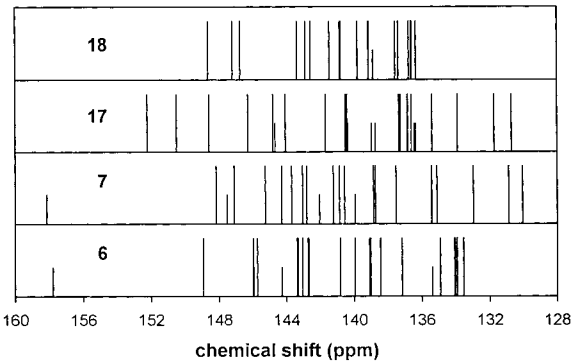

Figure 7. Theoretical ^{13}C NMR spectra of C_{2v} isomers of fullerene C_{84} labeled by isomer number.[7]

isomer **21**. The difference between the calculated NMR spectra of isomers **5** and **21** is less marked, making the identification difficult.

C. C_2 Isomers. Five isomers, **2**, **8**, **9**, **11**, and **13**, have C_2 symmetry and show 42 NMR peaks with equal intensity. Among the five isomers, isomer **11** has relatively low energy (8.39 kcal/mol) and a relatively high HOMO−LUMO gap (1.64 eV), indicating that it is the most stable C_2 isomer. All other isomers, **2**, **8**, **9**, and **13**, have energy values higher than 20 kcal/mol, and isomers **8**, **9**, and **13** also have HOMO−LUMO gaps that are lower than 1.3 eV.

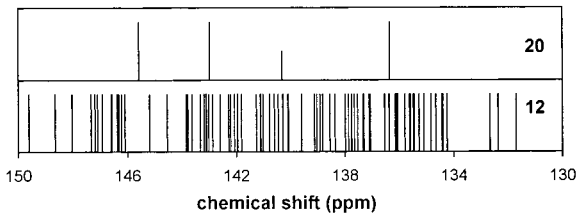

Figure 8. Theoretical ^{13}C NMR spectra of T_d and C_1 isomers of fullerene C_{84}, labeled by isomer number.[7] Spectra adjusted so that all full-intensity peaks appear at the same height.

One C_2 isomer has been observed experimentally.[14] The above energetic argument strongly suggests that this is isomer **11**. More importantly, the calculated NMR spectra of C_2 isomers give the conclusive evidence. Figure 4 compares the calculated NMR spectra of the C_2 isomers and the experimental result. The calculated spectral span of isomer **11**, 15.15 ppm, is in excellent agreement with the experimental span of the C_2 isomer, 15.13 ppm. Whereas the nearly perfect agreement of the numerical values is probably only a coincidence, other isomers have significantly larger spectral spans. For the chemical shifts, our DFT calculation was able to resolve the three groups of NMR peaks for isomer **11**, each containing 5, 5, and 32 peaks from downfield to upfield. The general trend stated earlier[25−27] and above lends us further confidence to believe that these groups correspond to the experimental data.

The predicted NMR spectra of isomers **2**, **8**, **9**, and **13** are also shown in Figure 4, showing different spectral spans and peak distributions.

D. C_s Isomers. Five IPR isomers of C_{84}, **3**, **10**, **14**, **15**, and **16**, have topological C_s point-group symmetry. Isomer **10** is predicted as a first-order saddle point at the B3LYP/STO-3G level of theory, thus, is not included in the high level calculations. Among the other four C_s isomers, the ratios of the number of full-intensity peaks to the number of half-intensity peaks are 40:4 for isomers **3** and **15** and 41:2 for isomers **14** and **16**.[7] Experimentally, two C_s isomers denoted as C_s(a) and C_s(b) have been observed,[13] and their ratios of full-intensity−half-intensity peak numbers indicate that they are isomers **14** and **16**, although unambiguous assignment could not be reached. The spectral ranges of isomers C_s(a) and C_s(b) are 134.11∼148.22 and 132.93∼148.44 ppm, respectively; thus, the spectral spans are 15.29 and 15.51 ppm, respectively. Because the 41 full-intensity peaks appear within the narrow spectral range, the only feature that will distinguish these two isomers lies in the position of the two half-intensity peaks.

Our theoretical NMR spectra calculated by DFT are able to give correct spectral spans and ranges for isomers **14** and **16**, as shown in Figure 5. The half-intensity peaks are predicted at 132.22 and 148.49 ppm for isomer **14**, which match the experimental values of C_s(b), 134.33 and 148.44 ppm, very well. For isomer **16**, the half-intensity peaks are at 136.12 and 141.01 ppm, matching the experimental values 137.03 and 141.76 ppm for C_s(a). This allows us to identify the C_s(b) isomer as isomer **14** and the C_s(a) isomer as isomer **16**.

The NMR spectrum of isomer **3** is predicted to have the widest range, 104.73∼160.85 ppm, among the C_{84} isomers. Because this isomer has a very high energy and small HOMO−LUMO gap, it is very unstable. On the other hand, isomer **15** has a relatively low energy and relatively large HOMO−LUMO gap; therefore, it might be obtained soon. The calculated NMR spectrum of isomer **15** exhibits a normal range for fullerenes.

E. D_{3d} and D_{6h} Isomers. Isomers **19** (D_{3d}) and **24** (D_{6h}) have been observed in a mixture that also contains other isomers[4a] and in a mixture that contains only these two isomers.[13] In our calculations, isomers **19** and **24** are less stable than isomer **23** by about 10.10 and 7.08 kcal/mol, respectively. The HOMO−LUMO gaps of isomers **19** and **24** are 1.39 and 2.34 eV, respectively, the former of which is relatively small but still comparable to that of the observed isomer **2** of fullerene C_{80},[27] a stable isomer. Thus, both the energy and HOMO−LUMO gap suggest isomers **19** and **24** to be relatively stable. Isomer **19** has six full-intensity peaks plus two half-intensity peaks. When compared with experimental NMR spectra[13] in Figure 6, our theoretical results show discrepancies that are much larger than the above cases and other assigned fullerene isomers, C_{70}, C_{76}:1, C_{78}:1∼3,[26] C_{80}:2,[27] and C_{82}:3.[28] Our calculation suggests that the two half-intensity peaks should appear at around 134 and 137 ppm, whereas they occur at 136.39 and 147.81 ppm in the experiment.[13] Because of impurities in the experiment, we concur with Heine et al.[22] that the peak at 147.81 ppm was misassigned in the experiment. If this peak is reassigned, the agreement between the theoretical and experimental results would be improved. With the exception of the half-intensity peak, the general pattern of the full-intensity peaks seems to agree with the experiment, although the spectral span is enlarged in our calculation.

For isomer **24**, two full-intensity peaks and three half-intensity peaks are expected. Our calculation predicts the two full-intensity peaks at 140.10 and 146.95 ppm, which are in overall agreement with experimental values of 139.50 and 144.78 ppm. The three-half-intensity peaks are predicted in the 135∼141 ppm region, with one of the three-half-intensity peaks occurring at 148.14 ppm in the experiment.[13] Similar to the case of isomer **19**, this half-intensity peak is probably misassigned in the experiment because of the impurities. When the discrepancy between the theory and experiment is considered, a more detailed measurement on a possibly isomer-pure sample is desirable for isomers **19** and **24**.

F. C_{2v} Isomers. Four isomers, **6**, **7**, **17**, and **18**, of fullerene C_{84} have C_{2v} symmetry. The ratios of full-intensity to half-intensity peaks are 19:4 for isomers **6** and **7**, 18:6 for isomer **17**, and 20:2 for isomer **18**. None of these isomers have been observed, but they are predicted to have energies of 15∼22 kcal/mol and HOMO−LUMO gaps of 1.3∼2.0 eV, which make them somewhat promising to be observed in the future. Figure 7 shows the computed NMR spectra for isomers **6**, **7**, **17**, and **18**.

Both isomers **6** and **7** have a half-intensity peak at 158 ppm, and all of the other peaks occur below 150 ppm. The lowest chemical shift of isomer **6** occurs at 133.54 ppm, whereas for isomer **7**, it is at 130.04 ppm. Compared to the positions of half-intensity peaks for isomer **7**, the half-intensity peaks of isomer **6** appear at lower chemical shifts. If these two isomers become available, these differences may be used in their identification. In the early experiment on minor C_{84} isomers,[4a] a single peak was observed at 160.58 ppm and assigned to isomer **21**. The spectral range of our calculated NMR spectrum for isomer **21** is 132.33∼146.32 ppm, thus, effectively eliminating this assignment. On the other hand, the spectra of isomers **6** and **7** both have a single half-intensity peak appearing at around 158 ppm and all of the other peaks are below 149 ppm. This distinct feature makes us suspect that the observed single peak[4a] might be attributed to either isomer **6** or **7**.

On the basis of energy and HOMO−LUMO gap, isomer **18** is more stable than isomer **17**. The predicted NMR chemical shifts of isomers **17** and **18** have values that are normal for fullerenes.

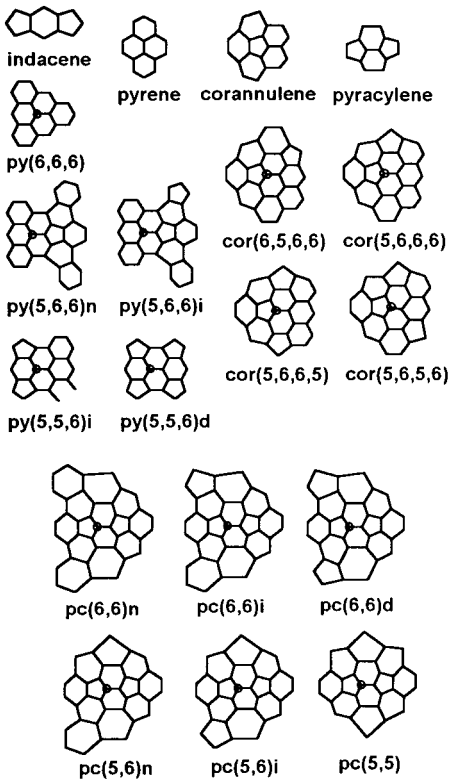

Figure 9. Structural motifs present in the nine observed IPR isomers of fullerene C_{84}.

G. T_d and C_1 Isomers. Isomer **20** has T_d symmetry and shows three full-intensity peaks plus one half-intensity peak. This isomer is predicted to have high energy. Isomer **12** has C_1 symmetry and shows 84 peaks with equal intensity. This isomer should be relatively stable. The predicted NMR spectra of isomers **20** and **12** are compiled in Figure 8. Both isomers have normal spectral ranges.

Chemical Shift and Local Geometry. Local connectivity has been suggested to affect chemical shift. Three types of carbon sites, the pyracylene (pc) site, the corannulene (cor) site, and the pyrene (py) site, as shown in Figure 9, were used to categorize the carbon atoms in fullerenes[39,40] and their chemical shifts should have the order pc > cor > py. Heine et al.[22] used the site concept in combination with the π-orbital axis vector (POAV) angle,[41] which measures the nonplanarity of the immediate environment of an sp^2 carbon, to correlate the calculated chemical shift and local geometry. Using the data for fullerenes C_{70}, C_{76}, and C_{78} and five isomers of C_{84}, a roughly linear relationship was reported for the pc and cor sites in their study, whereas no obvious relationship was indicated for the py sites. In a previous study,[26] we utilized the same scheme on fullerene isomers C_{70}, C_{76}:1, C_{78}:1~3, C_{84}:22, and C_{84}:23 and found that the POAV angles are mainly determined by connectivity, but chemical shifts show no apparent relationship with POAV angles. The lack of a linear relationship between chemical shift and POAV angle in the previous studies might be related to the fact that isomers of several fullerenes were included. The current identification of nine isomers of C_{84} gives us an opportunity to reevaluate this relationship.

The predicted chemical shifts of the observed nine isomers of C_{84}, **4**, **5**, **11**, **14**, **16**, **19**, and **22**−**24** are plotted against the POAV angle in Figure 10, where squares, crosses, and circles are used for py, cor, and pc types of atoms, respectively. This graph is very similar to the corresponding figure in ref 22 and closely resembles Figure 10 in ref 26 in several ways. First, with the exception of a few outliers, most POAV angles are within the 6.5~12.5° range, whereas most chemical shifts are within 132~150 ppm. Second, different carbon sites show different ranges of POAV angles, which are similar to the earlier case.[26] Type pc has a POAV angle range of 10.5~12.5°, type cor has a 9.0~11.5° range, and type py has a 6.5~9.0° range. Finally, the previously observed chemical shift range for each type of carbon seems to present here: 132~152 ppm for type

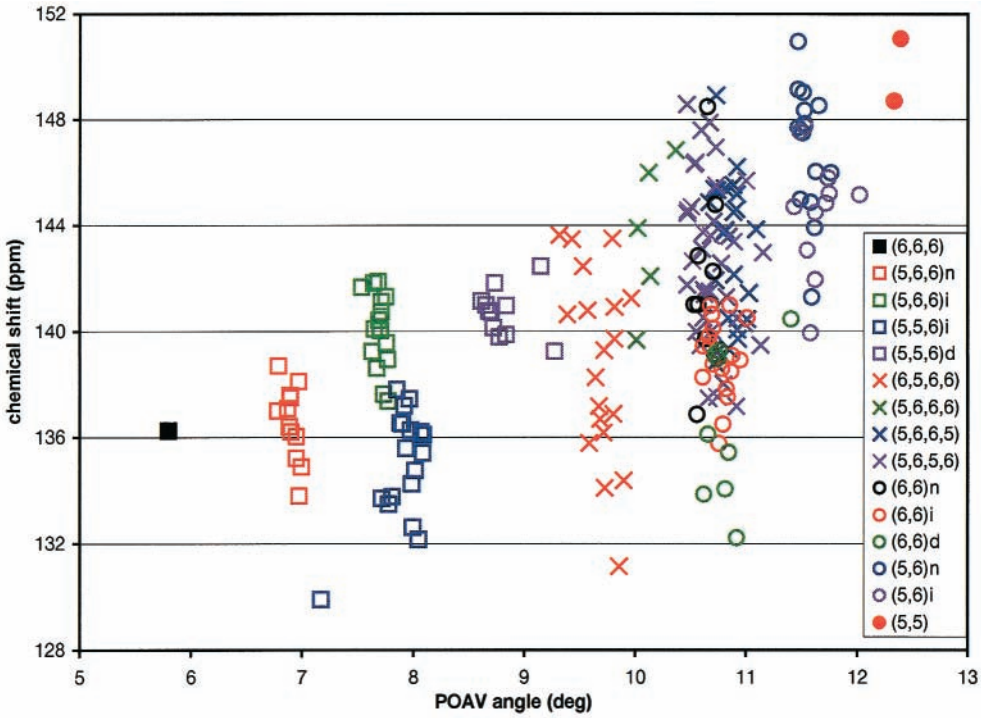

Figure 10. Theoretical ^{13}C NMR chemical shifts and POAV angles of isomers **4**, **5**, **11**, **14**, **16**, **19**, and **22**−**24** of fullerene C_{84} calculated by B3LYP/6-31G*. The py type carbons are represented by squares, the cor type by crosses, and the pc type by circles.

pc, 131∼149 ppm for type cor and 130∼143 ppm for type py. Although no strict linear relationship is obvious, the chemical shift generally increases when the POAV angle increases.

Another reason for the lack of a linear relationship between chemical shift and POAV angle might be the effect of farther neighbors that differentiate among the different py sites, cor sites and pc sites. Here we consider the connectivity of an expanded range. For a py type carbon atom, the three fused rings are all six-membered rings. Each of the three bonds connects to a ring that could be either a six-membered or a five-membered ring. This leads to three types of environments, (6,6,6), (5,6,6) and (5,5,6). By inspecting the chemical shifts of these three types of carbon atoms, it turns out that if the five-membered ring of the latter two types forms an s-indacene type of motif with another five-membered ring, POAV angles and chemical shifts show characteristic values. This scheme leads to a total of five different motifs that exist in the nine isomers of C_{84} for py type carbon. The five motifs are shown in Figure 9. The -n, -i, and -d suffix in the notation means no, one, and two s-indacene motifs, respectively. Distinct ranges of POAV angle and chemical shift can be clearly seen for each of the five motifs in Figure 10, as represented by the five distinct groups of squares. An outlier occurs at a POAV angle and chemical shift that are lower than the normal values for the py-(5,5,6)i type. This atom is connected to the only atom that is of the py(6,6,6) type in our data set. Except the single outlier, the second neighbor connectivity gives five types of atoms that have characteristic chemical shift and POAV angle for the py type carbons.

For the cor and py types, further neighbors need to be considered. A total of four motifs exist for cor type atoms in the nine C_{84} isomers and a total of six motifs for pc type atoms. Figure 9 shows all of these motifs. Although the ranges of POAV angle and chemical shift for these motifs are less distinguishable than for the motifs of py carbons, two and three groups of carbon sites exist for cor and pc carbon, respectively. For cor type carbon, the existence of a five-membered ring on one side or both sides gives different POAV angles, whereas the chemical shift ranges of the two groups overlap. For pc type carbons, the data points form three groups according to the existence of no five-membered ring, one five-membered ring, or two five-membered rings around the original pyracylene motif. Each of these groups has a characteristic range for the POAV angle, but the chemical shifts appear over large overlapping ranges. Again, the -n, -i, and -d notations are used for pc type carbons to show the presence of the s-indacene motif between the five-membered ring in pyracylene and an adjacent five-membered ring. However, the formation of the s-indacene motif seems to have limited effect on these carbon sites because of the large distance relative to the carbon being observed.

Overall, fifteen motifs result from considering further connectivity in the nine observed isomers of C_{84}. These motifs give distinct ranges of POAV angle and chemical shift for py type atoms, whereas others give overlapping ranges for cor and pc types atoms.

IV. Conclusion

In summary, the structures of IPR isomers of fullerene C_{84} are optimized with B3LYP/6-31G*. Using the GIAO method, ^{13}C NMR chemical shieldings are calculated. Besides the major isomers **22** and **23**, isomers **4**−**6**, **11**, **12**, **14**−**16**, **18**, **19**, **21**, and **24** are predicted to have relatively low energy and a relatively large HOMO−LUMO gap. For isomers that have been assigned unambiguously, isomers **4**, **22**, and **23**, the calculated chemical shifts show good agreement with experimental values. The calculated NMR spectra enabled us to distinguish between isomers possessing the same symmetry. The previously provisionally assigned isomers D_2(II), C_2, C_s(a), and C_s(b) are assigned as isomers **5**, **11**, **16**, and **14**, respectively. The calculated NMR spectra of isomers **19** and **24** show larger differences than the above isomers as compared with experimental data, which were obtained from samples containing their mixtures. Further experimental study using an isomer-pure sample would clarify this discrepancy. On the basis of the agreement on the isomers **4**, **5**, **11**, **14**, **16**, **22**, and **23**, we expect that the predicted spectra would facilitate the identification of the other isomers when they become available.

For the nine observed C_{84} isomers, the local geometry or POAV angle is mainly determined by the connectivity. The calculated chemical shifts generally increase when POAV angles increase but no strict linear relationship can be obtained. When further connectivity is considered, the py type sites show five distinct groups, each of which has a characteristic range of POAV angle and chemical shift. For cor and pc types, two and three groups of sites are found, respectively, and each of these groups has a characteristic range for POAV angle but not for chemical shift.

Acknowledgment. This work was partly supported by the National Science Foundation under grants CHEM-9802300 and CHEM-9601976.

References and Notes

(1) (a) Diederich, F.; Ettl, R.; Rubin, Y.; Whetten, R. L.; Beck, R.; Alvarez, M.; Anz, S.; Sensharma, D.; Wudl, F.; Khemani, K. C.; Koch, A. *Science* **1991**, *252*, 548. (b) Kikuchi, K.; Nakahara, N.; Honda, M.; Suzuki, S.; Saito, K.; Shiromaru, H.; Yamauchi, K.; Ikemoto, I.; Kuramochi, T.; Hino, S.; Achiba, Y. *Chem. Lett.* **1991**, 1607.

(2) Allen, K. M.; Dennis, T. J. S.; Rosseinsky, M. J.; Shinohara, H. *J. Am. Chem. Soc.* **1998**, *120*, 6681.

(3) (a) Piacente, V.; Palchetti, C.; Gigli, G.; Scardala, P. *J. Phys. Chem. A* **1997**, *101*, 4303. (b) Brunetti, B.; Gigli, G.; Giglio, E.; Piacente, V.; Scardala, P. *J. Phys. Chem. B* **1997**, *101*, 10715.

(4) (a) Avent, A. G.; Dubois, D.; Pénicaud, A.; Taylor, R. *J. Chem. Soc., Perkin Trans. 2* **1997**, 1907. (b) Hulman, M.; Pichler, T.; Kuzmany, H.; Zerbetto, F.; Yamamoto, E.; Shinohara, H. N. *J. Mol. Struct.* **1997**, *408/409*, 359. (c) Dennis, T. J. S.; Hulman, M.; Kuzmany, H.; Shinohara, H. *J. Phys. Chem. B* **2000**, *104*, 5411.

(5) Crassous, J.; Rivera, J.; Fender, N. S.; Shu, L.; Echegoyen, L.; Thilgen, C.; Herrmann, A.; Diederich, F. *Angew. Chem., Int. Ed. Engl.* **1999**, *38*, 1613.

(6) Fowler, P. W.; Manolopoulos, D. E. *An Atlas of Fullerenes*; Oxford University Press, Inc.: New York, 1995; pp 73−80.

(7) Manolopoulos, D. E.; Fowler, P. W. *J. Chem. Phys.* **1992**, *96*, 7603.

(8) Kikuchi, K.; Nakahara, N.; Wakabayashi, T.; Suzuki, S.; Shiromaru, H.; Miyake, Y.; Saito, K.; Ikemoto, I.; Kainosho, M.; Achiba, Y. *Nature* **1992**, *357*, 142.

(9) Manolopoulos, D. E.; Fowler, P. W.; Taylor, R.; Kroto, H. W.; Walton, D. R. M. *J. Chem. Soc., Faraday Trans.* **1992**, *88*, 3117.

(10) Taylor, R.; Langley, G. J.; Avent, A. G.; Dennis, T. J. S.; Kroto, H. W.; Walton, D. R. M. *J. Chem. Soc., Perkin Trans. 2* **1993**, 1029.

(11) Kikuchi, K.; Miyake, Y.; Achiba, Y. *Carbon Cluster News* **1994**, *2*, 34.

(12) Dennis, T. J. S.; Kai, T.; Tomiyama, T.; Shinohara, H. *Chem. Commun.* **1998**, 619.

(13) Tagmatarchis, N.; Avent, A. G.; Prassides, K.; Dennis, T. J. S.; Shinohara, H. *Chem. Commun.* **1999**, 1023.

(14) Dennis, T. J. S.; Kai, T.; Asato, K.; Tomiyama, T.; Shinohara, H.; Yoshida, T.; Kobayashi, Y.; Ishiwatari, H.; Miyake, Y.; Kikuchi, K.; Achiba, Y. *J. Phys. Chem. A* **1999**, *103*, 8747.

(15) Wang, G. W.; Saunders, M.; Khong, A.; Cross, R. J. *J. Am. Chem. Soc.* **2000**, *122*, 3216.

(16) Zhang, B. L.; Wang, C. Z.; Ho, K. M. *J. Chem. Phys.* **1992**, *96*, 7183.

(17) Bakowies, D.; Kolb, M.; Thiel, W.; Richard, S.; Ahlrichs, R.; Kappes, M. M. *Chem. Phys. Lett.* **1992**, *200*, 411.

(18) Schneider, U.; Richard, S.; Kappes, M. M.; Ahlrichs, R. *Chem. Phys. Lett.* **1993**, *210*, 165.

(19) Fowler, P. W.; Zerbetto, F. *Chem. Phys. Lett.* **1995**, *243*, 36.

(20) Bühl, K.; Wüllen, C. V. *Chem. Phys. Lett.* **1995**, *247*, 63.

(21) Nishikawa, T.; Kinoshita, T.; Nanbu, S.; Aoyagi, M. *THEOCHEM* **1999**, *461*−*462*, 453.
(22) Heine, T.; Bühl, M.; Fowler, P. W.; Seifert, G. *Chem. Phys. Lett*. **2000**, *316*, 373.
(23) Cioslowski, J.; Rao, N.; Moncrieff, D. *J. Am. Chem. Soc*. **2000**, *122*, 8265.
(24) Heine, T.; Seifert, G.; Fowler, P. W.; Zerbetto, F. *J. Phys. Chem. A* **1999**, *103*, 8738.
(25) Sun, G.; Kertesz, M. *New J. Chem*. **2000**, *24*, 741.
(26) Sun, G.; Kertesz, M. *J. Phys. Chem. A* **2000**, *104*, 7398.
(27) Sun, G.; Kertesz, M. *Chem. Phys. Lett.* **2000**, *328*, 387.
(28) Sun, G.; Kertesz, M. *J. Phys. Chem. A* **2000**, accepted.
(29) Becke, A. D. *J. Chem. Phys.* **1993**, *98*, 5648.
(30) Lee, C.; Yang, W.; Parr, R. G. *Phys. Rev. B* **1988**, *37*, 785.
(31) Cheeseman, J. R.; Trucks, G. W.; Keith, T. A.; Frisch, M. J. *J. Chem. Phys*. **1996**, *104*, 5497.
(32) Wolinski, K.; Hinton, J. F.; Pulay, P. *J. Am. Chem. Soc*. **1990**, *112*, 8251.
(33) Frisch, M. J.; Trucks, G. W.; Schlegel, H. B.; Scuseria, G. E.; Robb, M. A.; Cheeseman, J. R.; Zakrzewski, V. G.; Montgomery, J. A., Jr.; Stratmann, R. E.; Burant, J. C.; Dapprich, S.; Millam, J. M.; Daniels, A. D.; Kudin, K. N.; Strain, M. C.; Farkas, O.; Tomasi, J.; Barone, V.; Cossi, M.; Cammi, R.; Mennucci, B.; Pomelli, C.; Adamo, C.; Clifford, S.; Ochterski, J.; Petersson, G. A.; Ayala, P. Y.; Cui, Q.; Morokuma, K.; Malick, D. K.; Rabuck, A. D.; Raghavachari, K.; Foresman, J. B.; Cioslowski, J.; Ortiz, J. V.; Stefanov, B. B.; Liu, G.; Liashenko, A.; Piskorz, P.; Komaromi, I.; Gomperts, R.; Martin, R. L.; Fox, D. J.; Keith, T.; Al-Laham, M. A.; Peng, C. Y.; Nanayakkara, A.; Gonzalez, C.; Challacombe, M.; Gill, P. M. W.; Johnson, B. G.; Chen, W.; Wong, M. W.; Andres, J. L.; Head-Gordon, M.; Replogle, E. S.; Pople, J. A. *Gaussian 98*, revision A.5; Gaussian, Inc.: Pittsburgh, PA, 1998.
(34) *PQS*, version 2.1; Parallel Quantum Solutions: Fayetteville, AR, 1998.
(35) Khon, W.; Sham, L. J. *Phys. Rev.* **1965**, *140A*, 1133.
(36) Baerends, E. J.; Gritsenko, O. V. *J. Phys. Chem.* **1997**, *101*, 5383.
(37) Stowasser, R.; Hoffmann, R. *J. Am. Chem. Soc.* **1999**, *121*, 3414.
(38) Aihara, J. *Theor. Chem. Acc.* **1999**, *102*, 134.
(39) Ettl, R.; Chao, I.; Diederich, F.; Whetten, R. L. *Nature* **1991**, *353*, 149.
(40) Diederich, F.; Whetten, R. L. *Acc. Chem. Res*. **1992**, *25*, 119.
(41) Haddon, R. C.; Scott, L. T. *Pure Appl. Chem*. **1986**, *58*, 137.